12.5% EFFICIENT RGS SILICON SOLAR CELLS WITH CARRIER COLLECTING CHANNELS

Giso Hahn[1], Christian Haessler[2], Martin Langenkamp[3]
[1]*Universität Konstanz, Fachbereich Physik, Fach X916, 78457 Konstanz, Germany*
Tel.: +49-7531-88-3644, Fax: +49-7531-88-3895
E-mail: giso.hahn@uni-konstanz.de
[2]*Bayer AG, Rheinuferstr. 7-9, 47829 Krefeld, Germany*
[3]*MPI für Mikrostrukturphysik, Weinberg 2, 06120 Halle, Germany*

ABSTRACT: The RGS wafer technology has a high potential to reduce Wp costs in photovoltaics. But the advantage of a very fast production technique has to be faced with a high amount of crystal defects resulting in small diffusion lengths. Therefore the solar cell process has to be adapted to the material in order to reach satisfactory efficiencies.
A mechanical V-texture provides higher short circuit currents and efficiencies mainly because of an increased carrier collection probability. Efficiencies >10% can only be reached using bulk passivation by atomic hydrogen, which drastically improves cell performance. An optimised hydrogenation step in conjunction with a V-texture resulted in record efficiencies of 12.5%.
Another mechanism for a better current collection is a 3-dimensional network of dislocations. Oxygen precipitates at the dislocations are the cause for inversion of the p-type material and the dislocation acts as a prolongation of the surface emitter into the bulk. By this mechanism short circuit current densities >34 mA/cm^2 could be achieved despite of bulk lifetimes in the range of only 0.5 µs. Efficiencies of 12.5% have been obtained on material with a high and low amount of current collecting channels.
Keywords: Ribbon Silicon - 1: Multi-Crystalline - 2: Passivation - 3

1. INTRODUCTION

RGS (Ribbon Growth on Substrate) silicon is a multicrystalline material for PV which makes use of all advantages originating from a horizontal ribbon growth technique as compared to currently available standard cast as well as vertical ribbon growth techniques. It is currently taking the step from laboratory development at Bayer AG to pilot production at ECN in Petten (Netherlands). Therefore, it is of great interest to investigate its properties and potential in efficiency in order to check its suitability in general of becoming the crystalline silicon material of the future allowing a significant reduction in the costs per Wp. This paper gives a survey of solar cell results obtained during the RGS laboratory development.

Within the past years the share of multicrystalline silicon within the global PV module market steadily increased and now contributes to the largest fraction of module shipment. Within this share the development of ribbon growth techniques is of special interest as several studies attest modules made from ribbon silicon solar cells the highest potential in cost reduction per Wp of all crystalline silicon materials, comparable to crystalline thin films (e.g. [1]). This is mainly due to the saving of silicon material bringing down the wafering costs (no slicing, no ingot casting) and using well known equipment currently available. The main difference between the RGS technique and other ribbon materials already being produced commercially at the moment (e.g. ASE America's EFG or Evergreen Solar's String Ribbon) is the very high production rate of RGS which allows pulling speeds of ~10 cm/s as compared to 1-2 cm/min for the other ribbons mentioned above. This advantage concerning wafering costs has to be met on the other hand with specific material properties caused by the crystallisation process.

2. RIBBON GROWTH ON SUBSTRATE SILICON

The principle of the RGS wafer fabrication technique [2] is shown in Fig. 1. Substrates are pulled underneath the molten silicon inside a casting frame. The wafer crystallises on the reusable substrate which absorbs the heat. Decoupling of crystallisation and pulling direction allows the very fast pull speeds despite of the slower crystallisation velocity. In the future a revolving belt of substrates provides a continuous fabrication of wafers. However, all RGS solar cells fabricated so far origin from a lab-scale R&D production machine built at Bayer AG for proof-of-principle reasons allowing the fabrication of 10 wafers subsequently in a run. Boron doped (1 Ω cm) p-type wafers from this machine contain a fairly high amount of oxygen and carbon (~2*10^{18} cm^{-3} and ~1*10^{18} cm^{-3}, respectively), have average grain sizes <1 mm and dislocation densities of 10^5-10^7 cm^{-2}. Therefore, as grown lifetimes are in the range of just 0.1 µs. The fact that this machine can never be run in thermal equilibrium makes solar cell process development a difficult task because wafers originating from different runs (10 wafers per run)

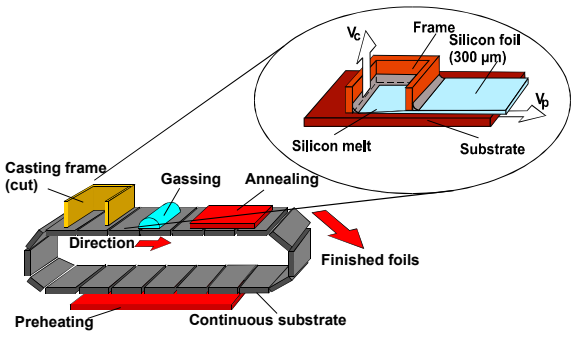

Figure 1: Principle of the continuous RGS wafer fabrication technique.

as well as wafers from the same run can not necessarily be compared with each other.

Bayer AG developed a special cooling sequence directly after crystallisation which allows the interstitial oxygen to precipitate at extended defects. In this way [O_i] is reduced to about $5*10^{17}$ cm^{-3} preventing the formation of recombination active New Donors [3] during the following high temperature steps in the cell process.

3. CELL PROCESS

The process for the fabrication of RGS solar cells developed at University of Konstanz is shown schematically in Fig 2. In its basic form it contains a mechanical levelling of the uneven wafer front surface using a conventional dicing saw followed by an acidic damage etch, a $POCl_3$ emitter diffusion (80 Ω/sq), front surface passivation using a thin dry thermal oxide, sintering of Al (evaporated) on the back side, followed by photolithography for front contact (Ti/Pd/Ag, evaporated) and Al evaporation for the back contact. After edge isolation by dicing cells (2x2 cm^2) are characterised. On the best cells a double layer antireflective coating (DARC) using ZnS/MgF_2 can be deposited.

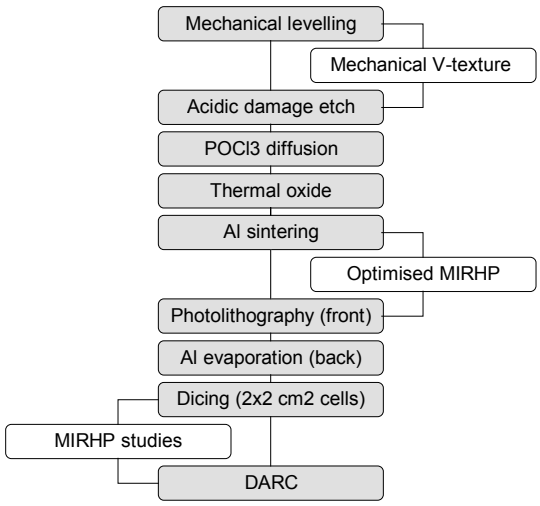

Figure 2: Process flow for the fabrication of RGS solar cells. The basic process is shown in the middle.

Maximum cell efficiencies reached for this basic process shown in the middle of Fig. 2 are in the range of 9%, limited by the high concentration of crystal defects present in the material. Diffusion lengths L_{diff} in the finished cell structure are <20 µm. From these results follows that processing has to be adapted to the material needs if L_{diff} as well as efficiency shall increase. Therefore several steps within the cell process have been investigated. Apart from gettering studies the focus has been laid on two methods which turned out to be successful in significantly enhancing efficiencies.

3.1 Mechanical V-texture

A macroscopic mechanical V-texture of the cell's surface can be of use in a threefold way: reflectivity is reduced, charge carriers are generated closer to the surface due to the inclined penetration of the light, and collection probability is enhanced because the distance charge carriers have to diffuse to the collecting emitter surface is reduced. These three effects sum up to an increase in efficiency of up to 8% relative for an L_{diff} as it is typical in RGS. A more detailed study is presented in [4].

The basic process was adjusted in order to implement a V-texture as an additional processing step. After levelling the surface was textured, again using a conventional wafer dicing saw with bevelled blades (Fig. 2). Efficiencies could be increased up to 10.0% with the V-texture implemented in the basic process.

3.2 MIRHP passivation

The passivation of crystal defects by atomic hydrogen using the microwave induced remote hydrogen plasma (MIRHP) method [5] turned out to be a key step in improving not only L_{diff} but all cell parameters drastically. Therefore detailed analysis of the MIRHP passivation step and its functioning in RGS material has been carried out. The hydrogenation step has to be implemented after dicing as visible in Fig. 2 (left), because only in this way the resulting effects can be measured directly on cell level. Several optimisation studies revealed that hydrogenation has a pronounced impact on cell parameters [6,7]. Apart from improvements in fill factor and V_{oc}, the internal quantum efficiency (IQE) in the long wavelength part is improved which is the result of an increased L_{diff}. One key result of the investigations is that H-passivation is slowed down in RGS due to the higher amount of interstitial oxygen as compared to other multicrystalline materials (e.g. [8]). Even after 10 h of passivation at T = 350 °C short circuit current density J_{sc} still improves, revealing that the passivation is not yet complete, whereas other ribbon materials like EFG can be totally passivated at the same temperature in <2 h. The effusion of hydrogen out of the cell is slowed down as well as compared to materials with lower [O_i].

Higher passivation temperatures or longer passivation times could not be applied in these investigations because the space charge region is damaged by indiffusion of metal from the front grid.

Using these results, an improved MIRHP passivation step was implemented in the process before front grid formation (Fig. 2, right). Efficiencies could be increased to 11.8 for untextured flat and up to 12.5% for V-textured surfaces. L_{diff} in these cells is in the range of 35 µm.

Table I: Results of RGS cells fabricated using processes from Fig. 2 and discussed in the text (best cells).
*independently measured at FhG-ISE, JRC Ispra

Process	**L_{diff} [µm]**	**V_{oc} [mV]**	**η [%]**
Basic (B)	<20	520	9.3
B+V-texture	<20	517	10.0*
B+MIRHP	35	570	11.8
B+V-texture+MIRHP	35	560	12.5*

4. CURRENT COLLECTING CHANNELS

4.1 Existence of current collecting channels

The data provided in Table I clearly marks the current limitation of the material: L_{diff} is too small to reach higher

efficiencies, even if an optimised hydrogenation step or a V-texture of the front surface is applied. Another reason for the low efficiency η is the presence of oxygen related precipitates formed during the cooling sequence (section 2) which reduce $[O_i]$ but also limit fill factor to values typically <74%.

Nevertheless, these precipitates which act as internal gettering sites during cooling down and at high temperature steps in the cell process can be used on the other hand to increase J_{sc} as it is shown in the following.

In Fig. 3 the mapped IQE at 905 nm for two RGS solar cells processed using the sequence given in Fig. 2 (right) is presented. Although the two cells have been processed identically, cell 1 seems to have a higher L_{diff}, whereas in cell 2 only some regions of apparently higher L_{diff} are visible. Mapped measurements of the minority charge carrier lifetimes τ_b however revealed that lifetimes are more or less identical and <1 µs in both cells. Therefore an additional current collecting mechanism must be present in most areas of cell 1 and to a lesser extent in some areas of cell 2.

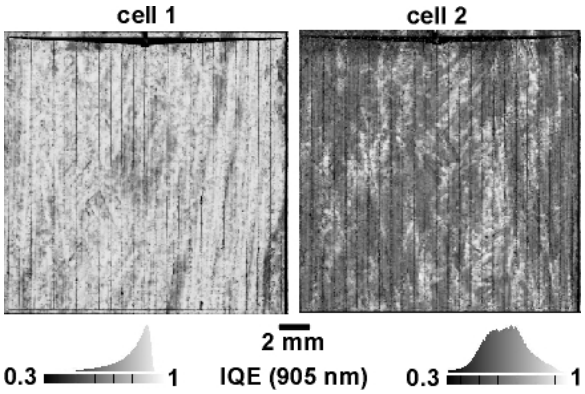

Figure 3: IQEs for two identically processed RGS solar cells with the same τ_b (<1 µs). In cell 1 an additional current collecting mechanism leads to very high IQEs despite of the small τ_b.

A special electron beam induced current (EBIC) measurement setup was chosen to clarify the nature of the current collection mechanism. For that purpose a cell showing this mechanism has been ground into a wedge shape and polished. The electron beam hit the cell's back side as it is shown in Fig. 4. The small L_{diff} should normally lead to a good EBIC contrast only in thin regions of the wedge. But also in areas with a remaining thickness of ~200 µm good EBIC contrast can be found. Fig. 4 (top right) shows a high resolution EBIC picture taken from such a thick part of the cell. Clearly visible are individual bright spots revealing a very efficient current collection. These spots coincide with etch pits caused by dislocations [9]. Fig. 4 (bottom) shows a cross sectional EBIC picture. Again visible is the efficient current collection throughout the whole bulk cell volume. If an n-type network of dislocations within the p-type base is linked to the front surface emitter, the high current collection could be explained.

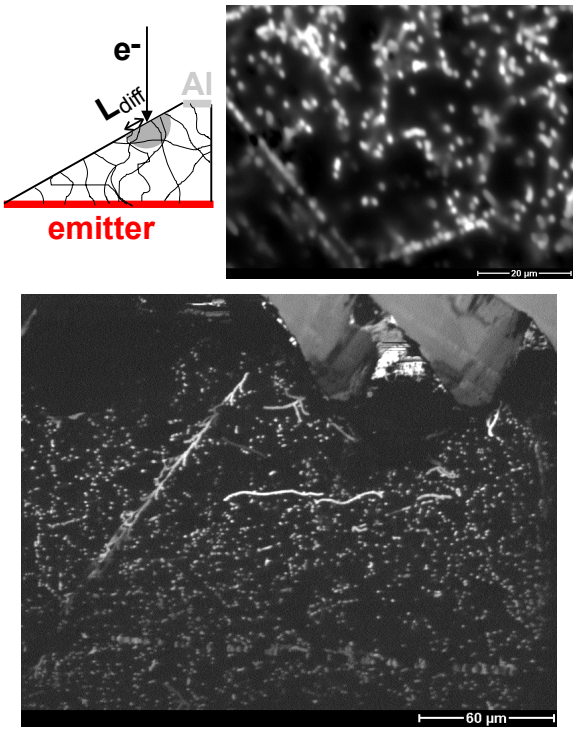

Figure 4: EBIC measurement of an RGS cell showing high IQE despite of a small L_{diff}. Top left: schematic setup for the measurement shown on the right revealing individual current collecting channels. Bottom: cross sectional EBIC demonstrating collection throughout the bulk cell volume.

A physical model of this current collection by inversion of p-type RGS material around dislocations is described in detail in [9]. There it could be shown that inversion around oxygen containing precipitates is possible. If these precipitates are densely packed along dislocation lines, a 3-dimensional link to the front surface emitter is given by the natural distribution of dislocations in the bulk. Spatially resolved secondary ion mass spectroscopy demonstrated that oxygen precipitates are present especially in areas of high IQE (channel regions) whereas in areas with lower IQE single precipitates can not be detected [10]. Additionally, transmission electron microscopy clearly demonstrated that dislocations in areas with high IQE are densely packed with precipitates, whereas in areas of lower IQE precipitates are present, but are not densely packed [10].

4.2 Influence on solar cell parameters

The influence of current collecting channels on solar cell performance is twofold: while the higher collection probability increases the IQE in the long wavelength part and therefore leads to a higher J_{sc}, fill factor (FF) is reduced by the presence of current collecting channels. One reason for the reduced FF is the enlarged and non-ideal space charge region caused by the 3-dimensional dislocation network. Additionally, shunting mechanisms can occur. Both effects are responsible for the fact that although J_{sc} is drastically enhanced, V_{oc} is not increased but slightly lowered. Dark IV-curves reveal a problematic second diode with ideality factors larger than 2, which can be explained within the proposed model [9].

The amount of current collecting channels present in the cell can be detected qualitatively by measuring the capacitance of the cell using low and high frequency, respectively [3]. A large difference between low and high frequency capacities indicates a slow charge carrier exchange that is contributing only to low frequency capacitance and is typical for minority charge carriers that are involved if collecting channels are present. By looking at the cell parameters of a whole set of RGS solar cells in dependency of the amount of channels present, it was found that FF decreases with increasing amount of channels while J_{sc} increases if more channels are present. The maximum efficiency however was not dependent on the amount of channels [10].

In Table II the cell parameters of the two cells from Fig. 2 are given. They represent the typical behaviour of RGS solar cells with a high (cell 1) and low (cell 2) amount of current collecting channels. Both cells are identically processed (V-textured surface, optimised MIRHP passivation) and result in the same record efficiency of 12.5%. While in cell 1 V_{oc} and especially FF are decreased, J_{sc} is largely enhanced by the presence of highly effective current collecting channels throughout the whole cell area. In this way J_{sc} >34 mA/cm^2 can be achieved although τ_b is well below 1 µs.

Table II: IV parameters (independently measured at JRC Ispra) of the best RGS solar cells processed so far.

	V_{oc} [mV]	J_{sc} [mA/cm^2]	FF [%]	η [%]
Cell 1	549	34.5	65.9	12.5
Cell 2	560	31.1	71.6	12.5

5. OUTLOOK

All RGS wafers used for solar cell processing so far have been fabricated using the lab-type non-continuous machine which is not run under thermal equilibrium conditions. Therefore material quality was not uniform from wafer to wafer. Stimulated by the results obtained using wafers from that machine a continuously operating RGS production machine is currently built-up at ECN (Netherlands). This machine will operate in thermal equilibrium and should supply a more homogenous wafer quality.

There are indications that the oxygen concentration can be reduced in RGS material using the new machine. This would simplify the fabrication process and increase FF. It has to be seen, if the current collection mechanism is still needed in this 'new' material for enhancing J_{sc}.

6. SUMMARY

RGS silicon has a high potential to reduce wafer costs drastically. Here the very fast production process is another advantage as compared to other already established ribbon techniques. Besides a high amount of extended crystal defects, high O and C concentrations are present. During the cooling sequence after crystallisation large oxygen precipitates are formed at extended defects like dislocations and [O_i] is reduced.

A mechanical V-texture can increase J_{sc} because of a higher charge carrier collection probability and efficiency is enhanced up to 8% relative.

The H-passivation of bulk defects using a remote plasma was found to be a key step for enhancing η to values >10%. An optimised hydrogenation step in conjunction with a V-textured surface led to efficiencies of 12.5% (2x2 cm^2).

J_{sc} can be further increased by making use of current collecting channels. These channels are formed around dislocations which are densely packed with O-precipitates formed during the cooling sequence after crystallisation. Inversion at these dislocations leads to a 3-dimensional extension of the front surface emitter into the silicon bulk. Therefore a very high J_{sc} (up to 35 mA/cm^2) is possible despite of a very low τ_b in the range of 0.5 µs.

Capacitance measurements revealed that FF is lowered with the number of channels increasing, therefore V_{oc} does not improve although J_{sc} is increased. The maximum efficiencies possible in present RGS material are not significantly influenced by the number of current collecting channels, as record efficiencies of 12.5% have been reached with cells showing a high and low amount of channels, respectively.

7. ACKNOWLEDGEMENTS

We like to thank Manfred Keil for assistance during solar cell processing and H.-U. Hoefs (Bayer AG) for stimulating discussions. This work was supported by the EC (JOR-CT 95-0030) and the German BMWi within the frame of the KoSi project (0329858J).

REFERENCES

[1] T.M. Bruton, J.M. Woodcock, K. Roy, B. Garrard, J. Alonso, J. Nijs, A. Raeuber, A. Vallera, H. Schade, E. Alsema, R. Hill, B. Dimmler, APAS study in: Music FM, publishable final EC project report.

[2] H. Lange, I. A. Schwirtlich, J. Cryst. Growth **104** (1990) 108.

[3] C. Haessler, H.-U. Hoefs, S. Thurm, O. Breitenstein, M. Langenkamp, Proc. 16th EC PVSEC, Glasgow, United Kingdom (2000) 1352.

[4] G. Hahn, C. Zechner, M. Rinio, P. Fath, G. Willeke, E. Bucher, J. Appl. Phys. **86** (12) (1999) 7179.

[5] M. Spiegel, S. Keller, P. Fath, G. Willeke, E. Bucher, Proc. 14th EC PVSEC, Barcelona, Spain (1997) 743.

[6] G. Hahn, C. Zechner, M. Spiegel, W. Jooss, P. Fath, G. Willeke, E. Bucher, Proc. 2nd WC PVSEC, Vienna, Austria (1998) 1840.

[7] M. Spiegel, G. Hahn, W. Jooss, S. Keller, P. Fath, G. Willeke, E. Bucher, Proc. 2nd WC PVSEC, Vienna, Austria (1998) 1685.

[8] T. Pernau, G. Hahn, M. Spiegel, G. Dietsche, Proc. 17th EC PVSEC, Munich, Germany (2001) to be published.

[9] O. Breitenstein, M. Langenkamp, J. P. Rakotoniaina, Solid State Phenomena **78-79** (2001) 29.

[10] G. Hahn, D. Sontag, C. Haessler, E-MRS 2001 Spring Meeting Strasbourg, to be published in Solar Energy Materials And Solar Cells.